



ELSEVIER

Journal of Chromatography A, 786 (1997) 117–124

JOURNAL OF
CHROMATOGRAPHY A

Intermolecular interactions in adsorbate–carbon systems of various nano- and adsorption textures

V.I. Zheivot*, E.M. Moroz, V.I. Zaikovskii, V.V. Chesnokov, V.Yu. Gavrilov

Boreskov Institute of Catalysis, Porspekt Akademika Laurentieva 5, Novosibirsk 630090, Russia

Received 17 September 1996; received in revised form 6 May 1997; accepted 7 May 1997

Abstract

Carbon materials possessing various nano- and adsorption textures have been investigated using adsorption, X-ray diffraction, electron microscopy and gas molecular chromatography. They were systematized according to their substructure characteristics and orientation of carbon layers. Substructure characteristics and carbon layer orientation essentially affect the adsorption and gas chromatography behavior of adsorbates. Carbons' application in molecular gas chromatography is discussed. © 1997 Elsevier Science B.V.

Keywords: Stationary phases, GC; Adsorbents; Carbon adsorbents; Hydrocarbons

1. Introduction

Two types of solids are used in gas molecular chromatography, i.e., supports of stationary liquid phases (gas–liquid chromatography) and adsorbents (gas adsorption chromatography).

Carbon materials form a particular class of adsorbents. Among them are activated charcoals [1], carbosieves [2,3], graphitized carbon blacks [4–6], carbon fibers [7,8] and carbon-containing adsorbents obtained via the catalytic decomposition of hydrocarbons [8,9] and carbonization of silica or alumina [10–12].

X-Ray phase analysis and electron microscopy of carbon materials allowed us to study these adsorbents profoundly and consider them more widely and systematize all carbons according to their nanotexture (substructure characteristics and carbon layer orientation).

In this regard we have investigated the effect of structure characteristics and carbon layer orientation in carbon nanotexture on their adsorption and gas chromatography properties.

2. Experimental

Carbon nanotexture can be described by substructure characteristics and the way in which the carbon layers are oriented. One of the main substructure characteristics is the graphitization degree, g , or the three-dimensional ordering degree. It determines the part of the hexagonal carbon layers packed like their packing in graphite crystal. Another characteristic is L_c – the packet thickness of the carbon layers along the c -axis. The graphitization degree was evaluated from the location of the 002 diffraction peak on an X-ray diagram. This spectral-line broadening determines the L_c value. We have evaluated g according to: $g = (d_{\text{disord.}} - d_{002}) / (d_{\text{disord.}} - d_{\text{graph.}})$ [13],

*Corresponding author.

where $d_{\text{disord.}} = 0.385$ is the interplanar space of disordered carbon structure.

Nanotexture has been established by X-ray diffraction and electron microscopy. In order to perform the X-ray phase analysis of carbons, we used an HZG 4/C X-ray diffractometer (FEB Freiburger Precision Mechanics) with Cu-anode and graphite plane reflected beam monochromator. The anode tube voltage and current intensity were 45 kV and 40 mA, respectively. The primary beam slits were 1 mm and 2 mm and reflected beam one was 0.25 mm.

Electron microscopy was carried out with a JEM 100 CX and JEM 2010 with a resolution of 0.14 nm. The carbon samples for the microscope were ultrasonically dispersed in ethanol and suspension drops were dried on "holey" carbon film.

The adsorption texture of carbon-containing materials was examined with an automated Digisorb-2600 (Micromeritics, USA) measuring nitrogen low-temperature adsorption isotherms.

Gas chromatography properties were studied using a Tswett chromatograph equipped with flame ionization detectors and stainless-steel columns. We have varied the column length from 50 cm up to 200 cm, the diameter was 2 mm. The carrier gas (nitrogen) velocity was $30 \text{ cm}^3 \text{ min}^{-1}$.

Specific ($V_{m,1}$) and absolute ($V_{A,1}$) retention volumes of various substances were measured for a small (zero) sample size. The peaks of adsorbates studied were practically symmetrical and the retention times were almost independent of the sample size. The measured temperature interval was varied against carbons studied. We have investigated the graphitization carbon blacks, for example, at temperatures varying from 50°C up to 120°C . The temperature study of filamentous carbons, obtained via catalytic reactions, was carried out at the 250°C – 300°C temperature interval. The retention data were measured 7–10 times at each temperature for 6–10 temperatures. Thus we calculated the corresponding differential molar changes of internal energy, $-\Delta U_1$, on adsorption of compounds and their adsorption dynamic capacities, $V_{A,1}^{298}$ (absolute retention volumes of adsorbates at the trapping temperature, i.e. room temperature as a rule [14]). The value $-\Delta U_1$ was determined from the dependence of $\log V_{m,1}$ on $1/T$. The $V_{A,1}^{298}$ values were obtained from this dependence as well as by extrapolation of the plot obtained to the trapping temperature (25°C).

The ability of the carbon surface to participate in additional specific intermolecular interactions with the adsorbates was evaluated by $-\Delta U_{1,\text{specif}}$. [15].

Carbon-containing solids of various nano- and adsorption textures – such as laboratory-made graphitized carbon blacks (both thermal and acetylenic), carbon molecular sieves (carbosphere) (Alltech Associates,), carbon fiber (actylene) [16], charcoal SKT, laboratory-prepared carbon coated alumina obtained via the catalytic decomposition of propane–butane mixture (alumina + 40% C) [12] and a composite based on carbon fiber (90% actylene) and alumina (10% pseudoboehmite) [17] – have been studied. Carbon fiber pretreatment was carried out with mechanochemical activation using the planetary ball mill AGO-2 according to Ref. [18].

We have also investigated the gas chromatographic behavior of filamentous carbons obtained in Institute of Catalysis via methane decomposition on catalysts, containing ferromagnetic metals (Ni and Fe). These materials consist of the carbon filaments, whose macrostructure is formed by the hexagonal carbon layers set at various angles to the filament axis. In turn this angle is determined by the metal used in the catalysts. It ranges from 180° (C/Fe) for iron catalyst, 90° (C/Cu–Ni and sample N1239) for copper–nickel catalyst to 30 – 45° (C/Ni) for nickel catalyst.

Simultaneously the products of methane decomposition on copper–nickel catalysts obtained using mechanochemical activation (sample N1239) or sedimentation (C/Cu–Ni) [19], have been studied.






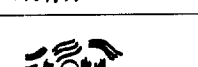





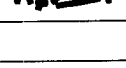
We have moreover investigated, carbons (C/Cu and C/Cu–Ni) modified, respectively, either by 5% (w/w) high boiling non-polar liquid phase such as OV-101 or via an additional deposition of the carbon upon divinyl catalytic decomposition.

3. Results and discussion

Table 1 shows the structure characteristics of the carbon materials obtained via X-ray diffraction and electron microscopy and their adsorption properties such as specific surface, S_{BET} and volume of micropores, V_{μ} .

Apparently, carbons have various graphitization degrees (g). The graphitized carbon blacks exhibit the highest (after graphite) values of g (e.g., for the

Table 1
Structural and adsorption characteristics of carbons

Carbon adsorbents	d_{002} (nm)	g	L_c (nm)	Carbon layers orientation	S_{BET} ($\text{m}^2 \text{g}^{-1}$)	V_{μ} ($\text{cm}^3 \text{g}^{-1}$)
1. Graphite	0.336	0.99	>100		–	–
2. Graphitized thermal carbon black (GTCB)	0.339	0.94	47		10	0
3. Acetylene carbon black	0.341	0.90	2.5		109	0
4. Catalytic carbon material (C/Fe)	0.340	0.92	12		67	–
5. Catalytic carbon material (C/Ni)	0.345	0.82	8.0		117	0
6. Catalytic carbon material (C/Cu–Ni)	0.349	0.73	6.8		118	0.007
7. Carbon fiber (actylene)	0.371	0.29	1.1		790	0.31
8. Carbon molecular sieves (carbosphere)	0.375	0.20	<1.0		890	0.34
9. Carbon composite material (90% actylene + 10% alumina)	0.360	0.51	1.1		1030	0.43
10. Carbon composite material (charcoal + alumina)	–	0	<1.0		–	–
11. Charcoal SKT	0.380	0.10	<1.0		–	–
12. Alumina +40% C	–	–	–		66	0

S_{BET} : Specific surface; V_{μ} : micropores volume; d : interplanar space; L_c : carbon layers thickness along c -axis.

thermal graphitized carbon black g equals 0.94). The activated charcoal (sample 11) and alumina coated with carbon via catalytic decomposition of propane–butane mixture (sample 12) have the lowest values of g . The products of methane decomposition using nickel (sample 5), copper–nickel (sample 6) catalysts occupy an intermediate position among the carbons studied (for C/Ni, $g=0.82$).

Note, that activated charcoal is X-ray amorphous ($g=0$). Carbon fiber (sample 7) and carbosieve

(sample 8) have more ordered structures: g values of these materials are 0.29 and 0.20, respectively.

Carbon fiber mechanical activation causes the ordering of actylene structure. As a result the graphitization degree of a new composite (sample 9) is twice as high as that of initial actylene. Such an increase in the graphitization degree of the carbon fiber is probably caused by intensive overheating of reactor during mechanochemical activation. For this reason, the micropore volume of actylene, subjected

to mechanical activation in air, also increases (see Table 1).

Fig. 1 presents an electron microphotograph of (C/Ni) sample consisting of carbon filaments. Here one can see one of the filament branches, whose macrostructure is formed by carbon layers set at an angle of about 30–45° to the filament axis. The filament is 50 nm in diameter and 10^4 nm long.

The carbon nanotexture of C/Cu–Ni is composed of carbon layers set at angles 90° and 30–45° to the filament axis.

The orientation of the hexagonal carbon layers in the nanotexture of the above samples is schematically presented by the drawings in Table 1 (samples 5 and 6).

Electron microphotographs of filamentous carbon C/Fe show another manner of carbon layer orientation (see Fig. 2). Here one can see (Fig. 2a) two types of carbon filaments. The first structure contains

chains of graphite globes. The globe size is 100 nm. They have cavities or contain iron inclusions.

The second structure contains the graphite filaments, 30–50 nm in diameter, whose symmetry axis coincides with the filament axis (see Fig. 2b).

The arrangement of the hexagonal carbon layers in the nanotexture of other materials, detected via electron microscopy and X-ray diffraction studies is also presented in Table 1.

The arrangement of the hexagonal carbon layers in the bulk of the nanotexture determines the surface texture of carbons and, hence, their adsorption and chromatographic properties.

In fact, the surface of graphitized carbon black is composed almost entirely of the basal faces of graphite crystal structure (see the drawing in Table 1), and it is practically planar [4,5].

As for the surface of C/Fe carbon, it consists mainly of the basal graphite crystal faces. However,

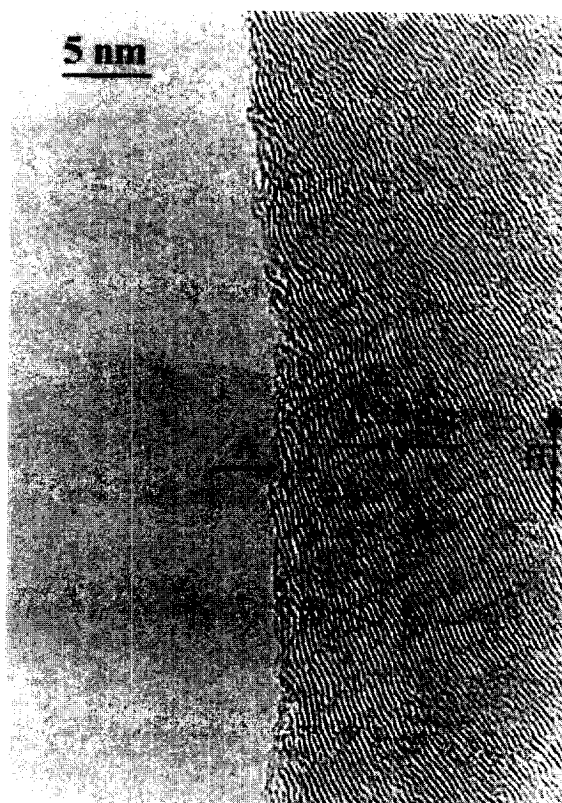


Fig. 1. Electron micrograph of the filamentous carbon obtained via methane catalytic decomposition using nickel catalyst (C/Ni): (A) the region of carbon structure distortion, (B) the filament axis.

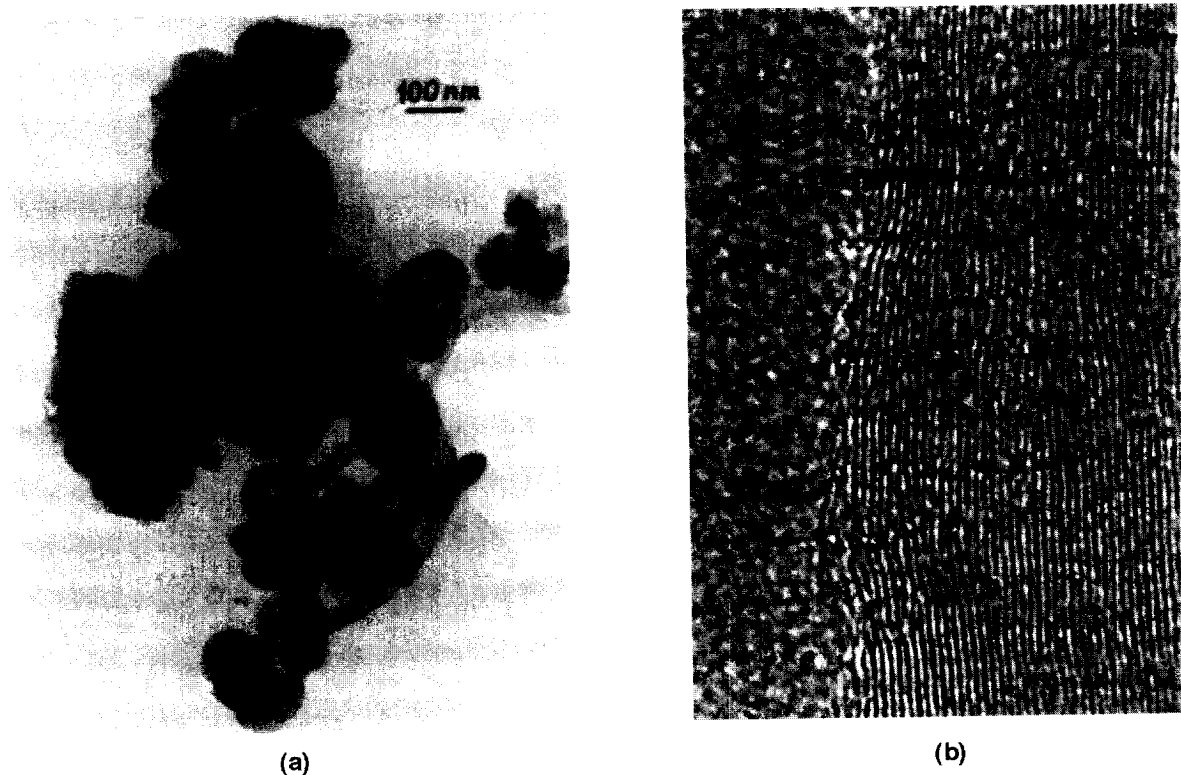


Fig. 2. Electron microphotographs of the filamentous carbon obtained upon catalytic decomposition of propane–butane mixture using iron catalyst (C/Fe); (a) two types of carbon filaments: (chains of graphite globes and graphite filaments with channel cavities); (b) the basal graphite crystal faces, set parallel to the filament axis A, with some defects near surface layer (in B region, for example).

this surface shows some defects, formed by surface carbon layers breaking, distorted carbon layers and lateral carbon atoms in the places of some graphite block joints.

The surface of carbon adsorbents with a high graphitization degree, obtained in catalytic methane decomposition (sample 5 and 6), consists of the lateral parts of basal graphite crystal faces. Therefore, the resulting adsorption potential of the external surface of catalytic carbons (C/Ni or C/Cu–Ni) most likely increases because of the energetically uncompensated state of the end carbon atoms in these nanotextures.

Indeed, comparison of $-\overline{\Delta U}_1$ for the *n*-alkane adsorption on carbon materials with various nanotexture (see Fig. 3) indicates that the adsorption ability of carbons such as C/Ni (curve 2), approaches, as expected, that of microporous carbons such as carbosieve (curve 1). However, the volume of micro-

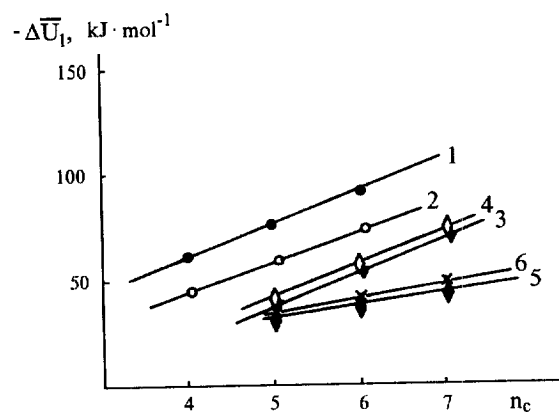


Fig. 3. $-\overline{\Delta U}_1$ dependences on the number of C atoms in an *n*-alkane molecule. (1) Carbosieve; (2) C/Ni; (3) C/Fe; (4) N1239, modified with 40% C; (5) graphitized thermal carbon black (GTCB); (6) acetylene carbon black.

pores, V_{μ} , for the former adsorbent is equal to zero, whereas V_{μ} for the latter is $0.34 \text{ cm}^3 \text{ g}^{-1}$ (see Table 1).

Note, that $-\overline{\Delta U}_1$ of sample C/Ni remains lower than that of carbo sieve. The lower values of $-\overline{\Delta U}_1$ in this case can be ascribed to the distortion of the carbon structure (see Fig. 1) due to the tendency of the end carbon atoms to compensate their excess energy. As a result, the lateral faces of some carbon packets close, especially within the 1–1.5 nm surface layer and the surface adsorption potential is lower than it should be.

Carbons with a planar surface (see curves 5 and 6 in Fig. 3) show the lowest adsorption towards *n*-alkanes: e.g., the $-\overline{\Delta U}_1$ for *n*-hexane adsorption on acetylene carbon black is 1.7 times lower than that on C/Ni.

Among the filamentous carbons C/Fe also possesses, as expected, the lowest adsorption ability (see curve 3). Only the modified filamentous carbons like the carbon obtained via additional carbon deposition on the Cu–Ni catalyst (sample N1239 + 40% w/w C) exhibit approximately the same adsorption ability (see curve 4) as the filamentous carbon, the nanotexture of which consists of carbon layers set parallel to the filament axis.

The gas chromatographic characteristics of the carbon adsorbents studied (see Table 2), show the same agreement.

Indeed, according to the data of Table 2, all adsorbates are better retained by the filamentous carbons than by the graphitized carbon blacks, the surface of which consists of basal graphite crystal faces.

Retention of adsorbates on the acetylene carbon black surface is 1–2 orders less than that on carbons

of which the surfaces consist of the lateral parts of basal graphite crystal faces.

Filamentous carbon like C/Fe, of which the carbon layers are arranged parallel to the filament axis (see Fig. 2b and Ref. [20]), retains adsorbates less efficiently than C/Ni or C/Cu–Ni.

Only if the latter two are respectively modified by a non-polar liquid phase such as OV-101 (sample C/Ni + 5% OV-101) or if additional carbon is deposited via divinyl catalytic decomposition (sample N1239 + 40% C), it is possible to obtain adsorbents of which the specific retention volumes approach that of C/Fe.

Note that modification of graphitized carbon blacks with a monolayer of practically non-polar liquid phase such as Apiezon L [21] or with a medium polar one such as 2,4-dinitrophenyl hydrazones of various ketones [21] decreases the specific retention volumes of *n*-alkanes by 1–2 orders in comparison with unmodified carbon blacks.

Such behavior of carbons like C/Ni after modification once again proves that filaments with various orientation of hexagonal carbon layers have a key effect on the gas chromatographic properties of carbon.

In addition, the active adsorption surface of filamentous carbons seems to contain more oxygen complexes than the planar surface of carbon because it comes into additional specific interaction with molecules, for example, of group B [4,5]. So, $-\overline{\Delta U}_{1,\text{specif.}}$ of benzene is 10 kDJ/mol for the filamentous carbon surface and 0 kDJ/mol for the planar surface.

Table 2 shows that carbons with the same chromatographic properties are obtained independently of whether mechanochemical activation or

Table 2
Specific retention volumes of various compounds on the carbons of different nanotextures at 250°C

Adsorbate	$V_{m,1} (\text{cm}^3 \text{ g}^{-1})$						
	Acetylene carbon black	C/Ni	C/Cu–Ni	N1239	N1239 + 40% C	C/Fe	C/Ni + 5% OV-101
1. <i>n</i> -Pentane	2.15	58.7	50.0	52.0	17.4	18.2	14.6
2. <i>n</i> -Hexane	5.44	300	264	270	99.1	100	59.2
3. <i>n</i> -Heptane	11.6	–	1534	1370	486	572	242
4. Benzene	4.05	84.9	79.0	80.5	32.0	30.6	25.4
5. Cyclohexane	–	280	275	271	67.0	84.1	72.4
6. Toluene	–	–	2100	1416	470	649	406

Table 3
Adsorption dynamic capacity of carbon adsorbents, $V_{A,1}^{298}$

Adsorbate	$V_{A,1}^{298}$ (cm ³ m ⁻²)		
	C/Ni	GTCB	Ambersorb XE-340 [22]
1. <i>n</i> -Pentane	$2.4 \cdot 10^6$	$1.1 \cdot 10^1$	$2.2 \cdot 10^3$
2. <i>n</i> -Hexane	$1.1 \cdot 10^8$	$1.0 \cdot 10^2$	$1.9 \cdot 10^5$
3. Cyclohexane	$2.6 \cdot 10^6$	$1.9 \cdot 10^1$	–
4. Benzene	$9.6 \cdot 10^7$	$5.9 \cdot 10^1$	$6.5 \cdot 10^1$
5. Toluene	$5.4 \cdot 10^6$	$1.6 \cdot 10^1$	$3.2 \cdot 10^3$
6. Chlorobenzene	$4.6 \cdot 10^4$	–	–
7. Acetone	$1.8 \cdot 10^2$	$2.5 \cdot 10^1$	3.2
8. Phenol	$1.2 \cdot 10^4$	$8.1 \cdot 10^2$	–

sedimentation were used (see sample N1239 and sample C/Cu–Ni, respectively).

As far as the dynamic adsorption capacities of various carbons are concerned, their values are given in Table 3. For catalytic carbons (e.g., C/Ni), these

values are by several orders higher than those for carbon adsorbents like graphitized thermal carbon black. Hence, carbons obtained via catalytic methane decomposition are promising for trapping *n*-alkanes, aromatic and cyclic hydrocarbons, phenols and chlorobenzene and can be used to determine their traces in environmental samples.

The higher adsorption ability of carbosieve (or actylene and composite obtained) (see Fig. 3 and Refs. [16,17]) towards light hydrocarbons allows to trap and to determine them at the ppm and parts of ppm level. So, actylene allows an increase in the sensitivity to C₁–C₄ hydrocarbons by 2–3 orders (in comparison to that reported in [22]). As a result, we have analysed snow sampled in the course of a search for new gas and oil deposits at the end of the Siberian winter. Together with the background peaks which are found in all snow samples, we have discovered some anomalies. Fig. 4 shows the background (a) and abnormal (b) chromatograms. These anomalies, which are associated with the influence of gas and oil deposits, allowed us to arrive at essential conclusions about their locations (analysis details will be published in Ref. [17]).

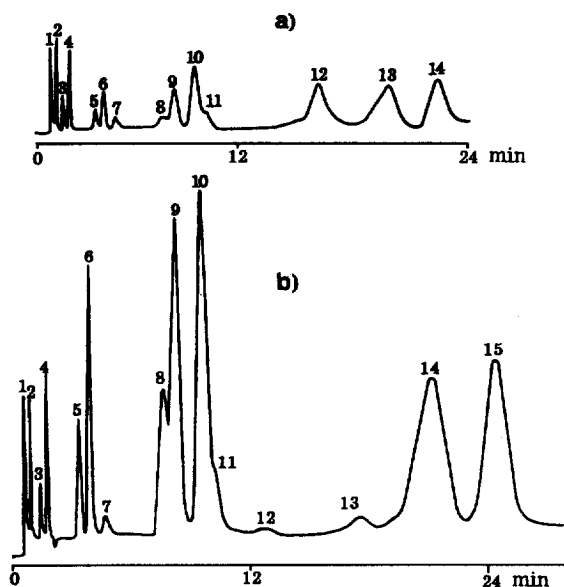


Fig. 4. Chromatograms of snow sampled in the course of a gas survey at Mansingyansk local raise the Jurassic deposits of which provided the oil in-flow: (a) background chromatogram and (b) abnormal chromatogram, which were obtained after solid-phase hydrocarbon extraction of melted snow (using as extractor actylene or new composite) followed by gas chromatography hydrocarbon analysis on-column (3 m×3 mm) with silica at temperatures programmed from ambient up to 150°C, with flame ionization detection. (1) Methane, (2) ethane, (3) ethene, (4) propane, (5) isobutane, (6) *n*-butane, (7) propene, (9) isopentane, (10) *n*-pentane, (15) *n*-hexane; other peaks are unidentified.

4. Conclusions

Systematization of carbons according to their nanotexture has been suggested. The effect of carbon nanotexture on the adsorption and gas chromatographic properties of sorbates has been studied. Carbons, whose surface is formed by the lateral parts of basal graphite crystal faces, give a retention of adsorbates 1–2 orders higher than that of carbons with a planar surface.

References

- [1] P.G. Jeffery and P.J. Kipping, Gas Analysis by Gas Chromatography, Pergamon Press, Oxford, New York, 1972.
- [2] T.N. Gvozdovich, A.V. Kiselev, Ya.I. Yashin, Neftekhimiya N8 (1968) 476.
- [3] R. Kaiser, Chromatographia 3 (1970) 28.
- [4] A.V. Kiselev and Ya.I. Yashin, Gas Adsorption Chromatography, New York, 1969; La Chromatographie Gas–Solid, Paris, 1969.

- [5] V.I. Zheivot, Proceedings of the 2nd International Conference on Carbon Black, Mulhouse, France, 1993, p. 61.
- [6] M.E. Shalaeva, V.I. Zheivot, V.B. Fenelonov, L.I. Fridman, V.V. Malakhov, *Zh. Anal. Khim.* 48 (1993) 1608.
- [7] V.I. Zheivot, E.M. Moroz, V.I. Zaikovskii, M.E. Shalaeva, A.A. Tsikoza, V.V. Malakhov, *Dokl. Akad. Nauk* 343 (1995) 781.
- [8] V.B. Fenelonov, L.B. Avdeeva, V.I. Zheivot, L.G. Okkel', O.V. Goncharova, L.G. Pimneva, *Kinet. Katal.* 34 (1993) 545.
- [9] A. Gierak, R. Leboda, D. Nazimek, *Chemia Anal.* N32 (1987) 957.
- [10] A. Gierak, R. Leboda, *J. Chromatogr.* 483 (1989) 197.
- [11] M.E. Shalaeva, V.I. Zheivot, N.A. Prokudina, V.V. Chesnokov, V.V. Malakhov, *Zh. Anal. Khim.* 51 (1996) 611.
- [12] V.I. Kasatochkin, A.T. Kaverov, *Dokl. Akad. Nauk* 117 (1957) 837.
- [13] C. Vidal-Madjar, M.F. Gonnord, F. Benchah, G. Guiochon, *J. Chromatogr. Sci.* 16 (1978) 190.
- [14] A.V. Kiselev, *Disc. Faraday Soc.* 40 (1965) 205.
- [15] V.I. Zheivot, M.E. Shalaeva, S.V. Danilenko, V.V. Malakhov, A.E. Kontorovich, *Zh. Anal. Khim.* 51 (1996) 592.
- [16] V.I. Zheivot, B.P. Zolotovskii, O.P. Klimova, *Zh. Anal. Khim.*, in press.
- [17] V.V. Chesnokov, V.I. Zaikovskii, R.A. Buyanov, V.V. Molchanov, L.M. Plyasova, *Kinet. Katal.* 35 (1994) 146.
- [18] O.V. Goncharova, L.B. Avdeeva, V.B. Fenelonov, L.M. Plyasova, V.V. Malakhov, G.S. Litvak, A.A. Vlasov, *Kinet. Katal.* 36 (1996) 293.
- [19] V.I. Zaikovskii, V.V. Chesnokov, R.A. Buyanov, *Appl. Catal.* 38 (1988) 41.
- [20] L.Ya. Gavrilina, O.A. Emelyanova, V.I. Zheivot, A.V. Kiselev, N.V. Kovaleva, *Kolloidn. Zh.* 40 (1978) 636.
- [21] G.A. Mogilevskii, F.A. Alekseev, N.V. Porshneva, K.P. Tokarev, M.S. Ton and B.S. Cherkinskaya, *Avtorskoe Svidetel'stvo, N269514, Bull. Isobretenii, N15* (1970) (Russian Patent).
- [22] G. Holzer, H. Shanfield, A. Zlatkis, *J. Chromatogr.* 142 (1977) 755.